INTERNATIONAL JOURNAL OF
COASTAL & OFFSHORE ENGINEERING
IJCOE No. 2/Spring 2016 (17-22)

Surveying sea surface effect in satellite altimeter-derived wind speed

Hossein Farjami[1], **Pavel Golubkin**[2], **Bertrand Chapron**[3]

[1]*Iranian National Institute for Oceanography and Atmospheric Science, IRAN*
[2]*Satellite Oceanography Laboratory, Russian State Hydrometeorological University, St. Petersburg, Russia,*
[3]*Laboratoire d'Oceanographie Spatiale, Ifremer, Plouzane, France*

ARTICLE INFO

Article History:
Received: 3 May. 2016
Accepted: 15 Jun. 2016

Keywords:
wind speed, satellite altimeter, coastal regions

ABSTRACT

To improve sea surface wind speed in coastal regions, we used nadir satellite altimeter measurements in the Persian Gulf and Arabian Sea. With combining normalized radar cross section for two bands of satellite altimeter measurements and significant wave height suggested the method to obtain "true" sea surface wind speed. In the coastal regions, we used a dimensionless significant wave height to gain empirical dependency to fetch-limited wind wave development. In this research, normalized radar cross section is simulated by using inverse wave age and fetch laws. As established this method helps to refine altimeter measurements of sea surface wind in the coastal regions.

1. Introduction

Satellite altimeters provide sea surface height and synchronous measurements of normalized radar cross section(NRCS) and significant wave height(Hs) in the oceans that related to sea surface state[1]. Most observations and analysis using global sampling of dual-frequency altimeters, i.e. since TOPEX measurements [2, 3], use both C- and Ku-band along with Hs estimates, and suggest means to better isolate the short-scale wind-related information contained in the differing NRCS measurements from the longer energy-containing scales [4, 5]. To better estimate of short surface wave scales by satellite altimeter measurements, we can use dual-frequency altimeter measurements. This waves directly related to physical air-sea processes, such as the local wind stress and the rate of gas exchange across the sea surface [6]. Elfouhaily et al. (1998) first proposed a theoretical method to estimate surface wind speed (U_{10}) from linear combinations of Ku- and C-band NRCS measurements of the TOPEX dual-frequency altimeter data. As demonstrated, the dual-frequency capability convincingly improves friction velocity estimation for wind speed higher than 7 m/s. Comparing with buoy data, the retrieved wind speed by a dual-frequency instrument was equally improved compared to a mono-frequency capability [4].

In this research, suggested the method to improve altimeter measurements of sea surface wind speed using nadir dual-frequency altimeter normalized and significant wave height measurements in the coastal areas, more precisely over the Persian Gulf and Arabian Sea. For our purpose, we use the Ocean Surface Topography Mission (OSTM)/Jason-2 and Jason-1 altimeter data. Of particular interest over coastal regions, the joint evolution of NRCS and Hs measurements can be analyzed and interpreted using fetch-limited laws to take into account possible rapid wind wave development [7, 8, 9].

Data and Methodology

The Ocean Surface Topography Mission on the Jason-2 satellite (OSTM/Jason-2) is a follow-on to the Jason-1 mission. It was launched in June 2008 in the frame of cooperation between National Aeronautics and Space Administration (NASA), European Organization for the Exploitation of Meteorological Satellites (Eumetsat), Centre National d'Etudes Spatiales (CNES), and National Oceanic and Atmospheric Administration (NOAA) with aims to continue high quality measurements of ocean parameters and to provide operational products to modeling and forecasting applications[10]. Main instrument carried aboard the satellite Jason-2 is Poseidon-3, which is a dual-frequency radar altimeter operating in Ku-band (13.575 GHz) and C-band (5.3 GHz). It has 9.9156 days repeat cycle with sample frequency 1Hz and 20Hz (http://www.aviso.altimetry.fr/). The second frequency is primarily used to provide correction for ionospheric electronic content. The data used in this study are Geophysical Data Records (GDRs) provided by NOAA.

Jason-1 satellite with a nadir-looking dual-frequency radar altimeter onboard was launched in December

2001. It operated with Ku-band and C-band frequencies the same as Jason-2 altimeter.

In the present study, (GDRs) Level-2 sampling from the Physical Oceanography Distributed Active Archive Center (PODAAC) of National Aeronautics and Space Administration (NASA) Jet Propulsion Laboratory (JPL) was used.

Longer waves not fully coupled to the local wind field can effect to altimeter measurements of wind speed[4]. This problem is especially relevant near coastal zones, where rapid wave development can take place under relatively constant offshore wind conditions. Growing waves contribute to broaden the local wind wave spectral range, leading to increase both the mean squared elevations and slopes of the ocean surface [7]. Probed along an altimeter track, such phenomena will thus lead to rapid and opposite Hs and NRCS changes. As a first consequence, derived wind speeds using a standard mono-frequency Ku-band algorithm, are likely to be underestimated [9].

To possibly overcome such a deficiency, Elfouhaily et al. (1998) proposed to analyze a more closely wind-related parameter $\delta\sigma^0_{dB} = (\sigma^0_C)_{dB} - (\sigma^0_{Ku})_{dB}$ to more efficiently isolate the short-scale roughness contribution. Here $(\sigma^0_C)_{dB}$ and $(\sigma^0_{Ku})_{dB}$ are NRCS of C- and Ku band in decibel, respectively, and $\delta\sigma^0_{dB}$ is their difference. Figure 2 (a) shows $(\sigma^0_{Ku})_{dB}$ and $(\sigma^0_C)_{dB}$, and their difference versus wind speed from Geophysical Data Records (*GDRs*) in the North Indian Ocean on 26 January 2013. Under homogenous sea state conditions, Ku- and C-band NRCS decrease with wind speed due to an increase of the surface wave Mean Square Slope (MSS). Not considering calibration issues, C-band NRCS are then expected higher than Ku-band ones, according to two effects: a larger C-band Fresnel coefficient, and a smaller effective MSS, linked to the larger C-band radar wavelength. Using NRCS difference, roughness impact, in the wavenumber interval confined by Ku- and C-band dividing wavenumbers, of order 285.6 and 112.2 rad/m, correspondingly, can be extracted. Since short-scale waves in this interval does not strongly depend on wave age, the use of the difference $\delta\sigma^0_{dB}$ shall be more closely related to wind speed only (see [3] for more details). In coastal regions and/or atmospheric fronts this parameter may thus be used to better interpret if rapid changes in altimeter-derived wind speed are caused by the impact of longer wave development under a relatively constant wind, or by "real" changes in wind speed conditions.

To further derive a more consistent local wind speed under nonhomogeneous conditions, e.g. fetch-limited situations, the altimeter Hs measurement and its evolution can further be considered. For closed-basin conditions over the Arctic area, Golubkin et al. (2014) [9] applied the concept introduced by Kitaigorodskii (1962) [13] to consider the self-similarity of wave development. Accordingly, knowing the distance from shore, the related Hs changes can also directly help to retrieve a wind estimate and the peak period of the developing wind sea. As further promoted by Badulin (2014) [8], a physical model for sea wave period from altimeter data can directly use Hs measurements and along-track spatial derivatives. Indeed, assuming stationary wind conditions, a simplified formulation can be derived from a physical model (Eq 6 in [8]), consistent with empirical fetch laws (see [14] and [15] for further discussions).

To illustrate these fetch-effects, we concentrate our analysis of altimeter measurements in the North Indian Ocean. In this paper, six particular altimeter passes are presented and discussed (Figure 1).

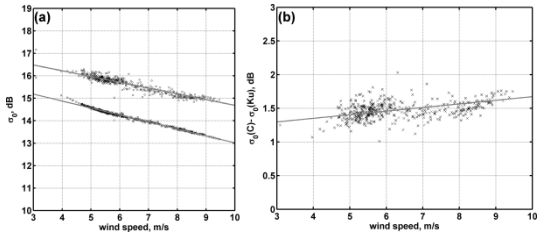

Figure 2. Jason-1 pass 45 on 26 January 2013

in the North Indian Ocean. (a) NRCS versus standard wind speed product for Ku- (crosses) and C-band (circles). (b) Difference between C-band and Ku-band NRCS. Gray lines show linear fit to the data

According to simplified physical optics or Kirchhoff approximation, we can estimate NRCS of satellite altimeter [2, 16]:

$$\sigma^0_{em}(0^\circ) = \frac{|R_0|^2}{MSS}\exp(-4k_r^2 h_s^2) \tag{1}$$

where R_0 is nominal Fresnel coefficient and $\exp(-4k_r^2 h_s^2)$ is a correction to the Geometrical Optics (GO) scattering approximation to take into account small (compared to the facet size) scale roughness impact, where k_r is radar wavenumber, h_s^2 the small scale variance in the wavenumber range $k > k_d$. The MSS and h_s^2 are calculated via wave spectrum as

$$MSS(\alpha, U_{10}, k_r) = \int_0^{k_d} B_0(\alpha, U_{10}, k)\, d\ln k \tag{2}$$

$$h_s^2 = \int_{k_d}^{\infty} k^{-2} B_0(\alpha, U_{10}, k)\, d\ln k \tag{3}$$

where k is wavenumber, B_0 is the omnidirectional wave saturation spectrum. U_{10} is wind speed at 10 m reference level, g is the gravitational acceleration, $\alpha = k_p^{1/2} U_{10} g^{-1/2}$ is the inverse wave age. Following a

2-scale PO scattering approximation, k_d corresponds to a typical scale linked to the facet size providing radar returns. For the sake of the demonstration, this typical scale is here taken as four times the radar wavelength. In the present study, we use the spectrum suggested by [17] with the following fetch law for inverse wave age:

$$\alpha = 0.84 \times \left\{ \tanh(\tilde{x} / \tilde{x}_0)^{0.4} \right\}^{-0.75} \quad (4)$$

Correspondingly, the integral over the wave spectrum provides the following fetch law for the dimensionless Hs:

$$\tilde{H}_s = 0.26 \times \tanh\left\{ \left(\tilde{x} / \tilde{x}_0 \right)^{0.4} \right\}^{1.25} \quad (5)$$

where $\tilde{x}$ is dimensionless fetch, $\tilde{x}_0 = 2.2 \times 10^{-4}$ and $\tilde{H}_s = H_s g / U_{10}^2$.

To help assess the interpretation of the observed NRCS changes along the altimeter tracks for the analyzed cases, we simulate NRCS, Eq. (1), taking into account the degree of development (wave age) via Eq. (4) for each fetch x. As an alternative, at each altimeter measurement, the inverse wave age, $\alpha = k_p^{1/2} U_{10} g^{-1/2}$, is evaluated using the altimeter Hs measurements from the relation (which follows from (4) and (5):

$$\alpha = 0.84 \times \left(\frac{\tilde{H}_s}{0.26} \right)^{-0.6} \quad (6)$$

The results of NRCS simulation are reported in Figure 3. The NRCS (Ku-band) is estimated for different wind speeds (5 m/s, 10 m/s, 15 m/s) as function of Hs. Very low Hs would thus correspond to very young sea states. To compare, the two-parameter model, NRCS(U10, Hs), proposed by[4], is also applied. As found, this two-parameter model seems to apply for relatively mature sea state conditions. For very young sea state conditions, it fails to reproduce the possible large NRCS increase. Correspondingly, altimeter wind speed will likely be underestimated. Accordingly, a more direct use of altimeter (NRCS, Hs) estimates and the corresponding joint (but opposite) NRCS and Hs gradients along the altimeter-track must be considered to help further constrain the estimation of the local wind speed and sea state degree of development.

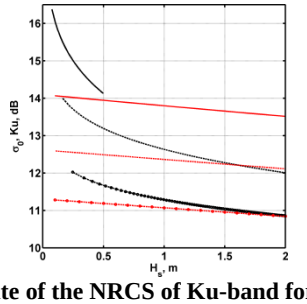

Figure 3. Estimate of the NRCS of Ku-band for wind speeds 5 m/s (solid line), 10 m/s (dashed line), 15 m/s (dash-dot line) as function of Hs. Black line calculated using model spectrum and red line calculated correspond to [4] algorithm.

Analysis and Results

In this part, different typical situations are reported to illustrate fetch-limited effects on satellite altimeter measurements. Jason-1 pass 45, January 26th 2013, is analyzed in the Arabian Sea from Kathiawar peninsula. In this case, the wind blows from coast and its direction is approximately aligned with the altimeter track. Figure 4 shows the evolution of Hs along the first 38 points from the coastline, corresponding to approximately 220 km between the first and the last measurements. Over this distance, the Hs grows from 0.5 m to approximately 1.5 meter (Figure 4a). Both Ku- and C-band NRCS also decrease with fetch. As expected, the altimeter wind speed derived from Ku-band NRCS is then constantly increasing with the distance from coast. However, the difference between C-band and Ku-band NRCS is found almost constant all along this altimeter segment (Figure 4b). As discussed above, this fact indicates that the wind speed is also likely constant (9.5 m/s) along the track, and the increase of altimeter wind speed results from the wave development.

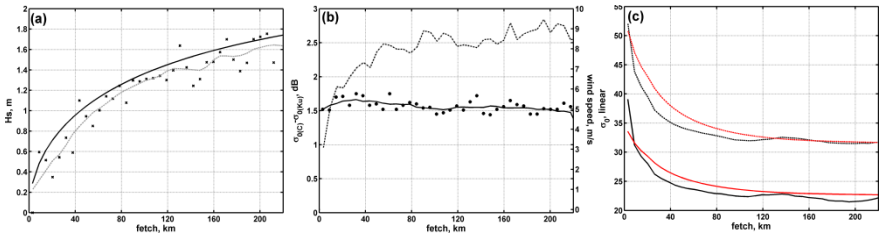

Figure 4. Jason-1 pass 45 on 26 January 2013 in the study region. (a) Hs measured by altimeter (symbols), smoothed Hs (dashed line) and calculated by using fetch law, Eq. 4, (solid line). (b) Difference between C-band and Ku-band NRCS (symbols) and their smoothed (solid line) and corresponding wind speed from the standard altimeter product (dashed line, right axis). (c) Smoothed NRCS measured by altimeter (black solid line for Ku-band and black dashed line for C-band) and calculated using model spectrum (red solid line for Ku-band and red dashed line for C-band), NRCS of model spectrum multiplied to 1.3 (for C-band) and 1.4 (for Ku-band) to fit with NRCS of altimeter measurement

Another example, on March, 17th 2014, Jason-2 pass 66 also captured a wave development condition in the Arabian Sea. Measurements are reported, Figure 5. In this case, the distance between the first and the last measurements corresponds to 180 km. Hs grows from 0.6 to 1.3 meters (Figure 5a) and the NRSC continuously drops over this interval. The standard altimeter wind speed thus increases from 4 to 8.4 m/s. The difference between NRCS for Ku- and C-band stays almost constant at 1.6 dB. As inferred using the fetch law, a 8.5 m/s constant wind speed can well describe the observed wave development.

On January 14th, 2010, Jason-1 pass 29, the altimeter wind speed increases from 5 to 8 m/s, over the 150 km segment. NRCS difference between Ku- and C-band ones is practically constant at 1.5 dB (Figure 6b). Hs grows from 0.6 to 1.6 meters, and using a constant wind speed 9.5 m/s can help interpret the measurements (Figure 6a).

On December 4th, 2010, Jason-1 pass 207, over 200 km, the difference between NRCS of Ku- and C-band measurements is almost constant, 1.5 dB, and Hs grows from 0.5 to 1.4 m (Figure 7a). Using a constant wind speed, 8.5 m/s, is then found to explain the altimeter observations.

Figure 8 and Figure 9 present two more examples to confirm the impact of wave development on altimeter measurements.

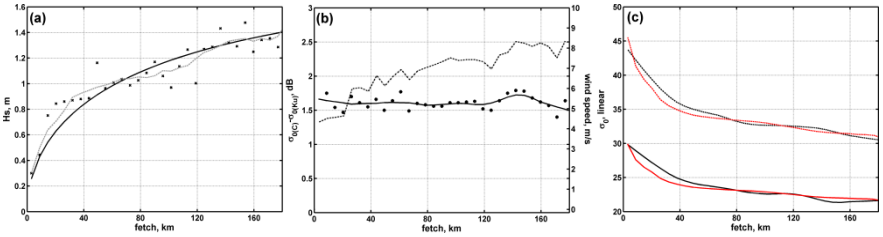

Figure 5. Same as in Figure 4 for Jason-2 pass 66 on 17 March 2014.

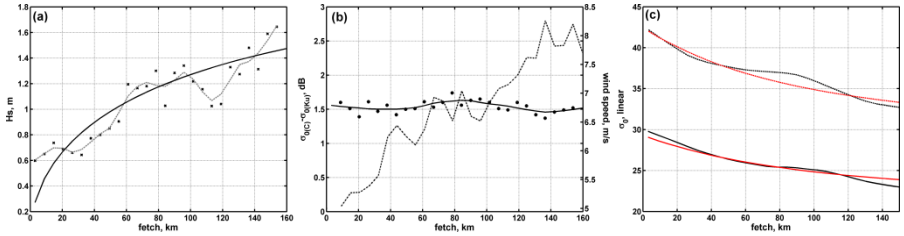

Figure 6. Same as in Figure 4 for Jason-1 pass 29 on 14 January 2010.

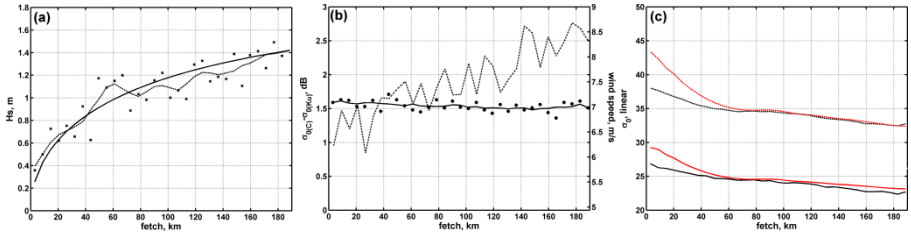

Figure 7. Same as in Figure 4 but for Jason-1 pass 207 on 4 December 2010.

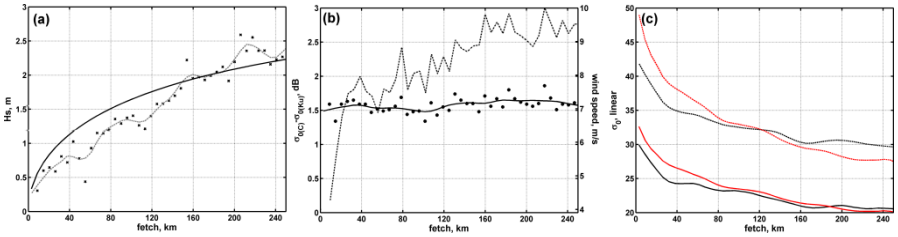

Figure 8. Same as in Figure 4 for Jason-1 pass 244 on 18 February 2005.

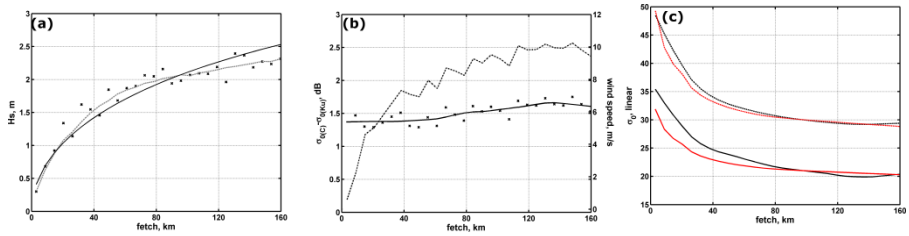

Figure 9. Same as in Figure 4 for Jason-1 pass 105 on 1 February 2004.

Discussion

As demonstrated, wind seas developing for these different cases seem to provide to broaden the local wind wave spectral range, leading to increase both the mean squared elevations and slopes of the ocean surface. From the different reported examples, the simplified NRCS model, Eq.(1), improved with Elfouhaily spectrum [17] with fetch laws (4) and (5) can reasonably explain the along-track altimeter observations. This approves the essential role of the wave development to interpret altimeter observation in coastal areas. As key to analyze and noticed for all these cases, the NRCS differences between Ku- and C-band, $\delta\sigma^0_{dB}$, take almost constant values along the analyzed altimeter tracks. This is related to the rapid modification of short scale roughness to the wind speed, and the weak impact of the sea state degree of development on this short scale roughness. Thus, a constant wind speed assumption can first be efficiently used for all considered cases, to further exploit the Hs changes to infer the most reasonable wind speed.

Golubkin, and et al. 2014, for closed-basin conditions, simply considered the largest retrieved wind values when using mono-frequency altimeter measurements (e.g., SARAL/AltiKa instrument). Using a dual-frequency instrument, the analysis is more straightforward, and can rely on the joint analysis of $\delta\sigma^0_{dB}$ and the Hs evolution.

Applications of satellite altimetry over the open ocean are certainly well established, but measurements near the coasts or in closed-basins [9], can necessitate more dedicated algorithm developments. This study has emphasized the potential of satellite altimeter measurements to derive more detailed sea state information in coastal regions. Indeed As demonstrated, analysis strategy and model developments can build on the combined the Ku- and C-band radar measurements, their difference, the measured significant wave height parameter and its along-track gradient.

With comparing Ku- and C-band NRCS measurements, along-track gradients and differences, can help to question the altimeter wind speed derived from a standard algorithm [3, 4]. Indeed, especially for coastal regions, when both along-track Ku- and C-band NRCS measurements are found to co-vary without major changes perceived in their differences, this likely indicates evolving sea state conditions. Persuasively, a further analysis of along-track altimeter Hs estimates and gradients can then help to more quantitatively confirm the sea state degree of development.

In this study, such developments of wind-driven waves were analyzed using self-similar wave theory [13, 17]. As expected and established using a simplified physical optics scattering model, NRCS and Hs along-track evolutions shall indeed be anti-correlated under developing sea state conditions. Based on the wave spectrum sea state dependency, simulations have been performed (Figure 3), and an empirical relation can be derived to describe this expected anti-correlation. Also, under stationary conditions, a simplified formulation can then further be derived to more efficiently estimate peak wave period information. Furthermore to the methodology proposed by [8], or the methodology based on empirical relationship [18] applied to assess coastal wave energy resource [19] the present analysis suggests to not only consider dual-frequency NRCS measurements [20], but also to analyze joint NRCS and Hs along-track gradients to more quantitatively constrain the peak wave period information. This subject will be studied in the future.

References

[1] Tournadre, J.; Chapron, B.; Reul, N. High resolution imaging of the ocean surface backscatter by inversion of altimeter waveforms. Journal of Atmospheric and Oceanic Technology, 2011, 28, 1050–1062. http://dx.doi.org/10.1175/2011JTECHO820.1.

[2] Chapron, B.; Katsaros, K.; Elfouhaily, T.; Vandemark, D. A note on relationships between sea surface roughness and altimeter backscatter. Remote Sensing and Global Modelling, 1995, 869-878.

[3] Elfouhaily, T.; Vandemark, D.; Gourrion, J.; Chapron, B. Estimation of wind stress using dual-frequency TOPEX data. Journal of Geophysical Research, 1998, 103, Issue C11, 25101–25108. http://dx.doi.org/10.1029/98JC00193.

[4] Gourrion, J.; Vandemark, D.; Bailey, S.; Chapron, B. Investigation of C-band altimeter cross section dependence on wind speed and sea state. Canadian Journal of Remote Sensing, 2002, vol. 28, issue 3, 484-489, http://dx.doi.org/10.5589/m02-046.

[5] Chen, G.; Chapron, B.; Ezraty, R.; Vandemark, D. A dual-frequency approach for retrieving sea surface wind speed from TOPEX altimetry. J. Geophys. Res., 2002, 107(C12), 322.

[6] Goddijn-Murphy L., Woolf , D.; Chapron, B.; Queffeulou, P. Improvements to estimating the air–sea gas transfer velocity by using dual-frequency, altimeter backscatter. Remote Sensing of Environment, 2013, Volume 139, 1–5. http://dx.doi.org/10.1016/j.rse.2013.07.026.

[7] Vandemark, D.; Chapron, B.; Sun, J.; Crescenti, G. H.; Graber, H. C. Ocean Wave Slope Observations Using Radar Backscatter and Laser Altimeters. J. Phys. Oceanogr., 2004, 34, 2825–2842.

[8] Badulin, S. I. A physical model of sea wave period from altimeter data. Journal Geophysical Research Oceans, 2014, 119, 856–869. http://dx.doi.org/10.1002/2013JC009336.

[9] Golubkin, P. A.; Chapron, B.; Kudryavtsev V. N. Wind Waves in the Arctic Seas: Envisat and AltiKa

Data Analysis. Marine Geodesy, 2014, http://dx.doi.org/10.1080/01490419.2014.990592.
[10] Dumont, J. P. OSTM/Jason-2 Products Handbook. 2015, JPL: STM-29-1237, NOAA/NESDIS: Polar Series/OSTM J400.
[11] Tomczak, M.; Godfrey, J. S. Regional Oceanography: an Introduction", 2nd edition, Elsevier Science Ltd., 2003, Oxford, U. K. ISBN: 817035068, 391pp.
[12] Rodo, X.; Comin, F. Global Climate Current Research and Uncertainties in the Climate System, 2002., Springer, Berlin, 10837865, 286 pp.
[13] Kitaigorodskii, S. A. Applications of the theory of similarity to the analysis of windgenerated wave motion as a stochastic process. Izv. Geophys. Ser. Acad. Sci., USSR 1, 1962, p105-117.
[14] Zakharov, V. E., Badulin, S. I., Hwang, P. A., Caulliez, G. Universality of sea wave growth and its physical roots, J. Fluid Mech., 2015, 780, 503–535, *doi:*10.1017/jfm.2015.468.
[15] Kudryavtsev, V.*;* Golubkin, P.*;* Chapron, B. A simplified wave enhancement criterion for moving extreme events, J. Geophys. Res. Oceans, 2015, 120, 7538–7558, *doi:*10.1002/2015JC011284.
[16] Kudryavtsev, V.; Akimov, D.; Johannessen, J.; Chapron, B. On radar imaging of current features: 1. Model and comparison with observations. J. Geophys. Res., 2005, 110, C07016, http://dx.doi.org/10.1029/2004JC002505.
[17] Elfouhaily, T.; Chapron, B.; Katsaros, K.; Vandemark, D. A Unified Directional Spectrum for Long and Short Wind-Driven Waves. Journal of Geophysical Research, 1997, 102, 15781–96. http://dx.doi.org/10.1029/97JC00467.
[18] Gommenginger, C. P.; Srokosz, M. A.; Challenor, P. G. Measuring ocean wave period with satellite altimeters: A simple empirical model, Geophys. Res. Lett., 2003, 30*(*22*), 2150, doi:*10.1029/2003GL017743.
[19] Goddijn-Murphy, L.; Martín Míguez, B.; McIlvenny, J.; Gleizon, P. Wave energy resource assessment with AltiKa satellite altimetry: A case study at a wave energy site. Geophysical Research Letter, 2015, 42, 5452–5459. http://dx.doi.org/10.1002/2015gl064490.
[20] Quilfen, Y.; Chapron, B.; Collard, F.; Serre, M. Calibration/validation of an altimeter wave period model and application to TOPEX/Poseidon and Jason-1 altimeters, Mar. Geod., 2004, 27*(*3–4*)*, 535–549, *doi:*10.1080/01490410490902025.